Mon. Not. R. Astron. Soc. **000**, 1–12 (2016) Printed 21 April 2016 (MN LATEX style file v2.2)

The peculiar Type Ia supernova iPTF14atg: Chandrasekhar-mass explosion or violent merger?

M. Kromer,[1⋆] C. Fremling,[1] R. Pakmor,[2] S. Taubenberger,[3,4] R. Amanullah,[5] S. B. Cenko,[6] C. Fransson,[1] A. Goobar,[5] G. Leloudas,[7,8] F. Taddia,[1] F. K. Röpke,[2,9] I. R. Seitenzahl,[10,11] S. A. Sim[11,12] and J. Sollerman[1]

[1]*The Oskar Klein Centre & Department of Astronomy, Stockholm University, AlbaNova, SE-106 91 Stockholm, Sweden*
[2]*Heidelberger Institut für Theoretische Studien, Schloss-Wolfsbrunnenweg 35, D-69118 Heidelberg, Germany*
[3]*European Southern Observatory, Karl-Schwarzschild-Str. 2, D-85748 Garching bei München, Germany*
[4]*Max-Planck-Institut für Astrophysik, Karl-Schwarzschild-Str. 1, D-85748 Garching bei München, Germany*
[5]*The Oskar Klein Centre & Department of Physics, Stockholm University, AlbaNova, SE-106 91 Stockholm, Sweden*
[6]*Astrophysics Science Division, NASA Goddard Space Flight Center, Mail Code 661, Greenbelt, MD 20771, USA*
[7]*Department of Particle Physics and Astrophysics, Weizmann Institute of Science, Rehovot 7610001, Israel*
[8]*Dark Cosmology Centre, Niels Bohr Institute, University of Copenhagen, Juliane Maries vej 30, 2100 Copenhagen, Denmark*
[9]*Zentrum für Astronomie der Universität Heidelberg, Institut für Theoretische Astrophysik, Philosophenweg 12, D-69120 Heidelberg, Germany*
[10]*Research School of Astronomy and Astrophysics, Australian National University, Canberra, ACT 2611, Australia*
[11]*ARC Centre of Excellence for All-Sky Astrophysics (CAASTRO)*
[12]*Astrophysics Research Centre, School of Mathematics and Physics, Queen's University Belfast, Belfast BT7 1NN, UK*

arXiv:1604.05730v1 [astro-ph.HE] 19 Apr 2016

Accepted, 20 April 2016. Received, 12 April 2016; in original form, 19 February 2016

ABSTRACT

iPTF14atg, a subluminous peculiar Type Ia supernova (SN Ia) similar to SN 2002es, is the first SN Ia for which a strong UV flash was observed in the early-time light curves. This has been interpreted as evidence for a single-degenerate (SD) progenitor system where such a signal is expected from interactions between the SN ejecta and the non-degenerate companion star. Here, we compare synthetic observables of multi-dimensional state-of-the-art explosion models for different progenitor scenarios to the light curves and spectra of iPTF14atg. From our models, we have difficulties explaining the spectral evolution of iPTF14atg within the SD progenitor channel. In contrast, we find that a violent merger of two carbon-oxygen white dwarfs with 0.9 and 0.76 $\mathrm{M}_{\odot}$, respectively, provides an excellent match to the spectral evolution of iPTF14atg from 10 d before to several weeks after maximum light. Our merger model does not naturally explain the initial UV flash of iPTF14atg. We discuss several possibilities like interactions of the SN ejecta with the circum-stellar medium and surface radioactivity from a He ignited merger that may be able to account for the early UV emission in violent merger models.

Key words: supernovae: individual: iPTF14atg – methods: numerical – hydrodynamics – radiative transfer – nuclear reactions, nucleosynthesis, abundances

1 INTRODUCTION

Despite the importance of Type Ia supernovae (SNe Ia) for cosmological distance measurements (Riess et al. 1998; Perlmutter et al. 1999) and decades of intensive work, their progenitors are still elusive. It is widely accepted that SNe Ia result from thermonuclear explosions in carbon–oxygen (CO) white dwarfs (WDs) that are triggered by some kind of interaction in a binary system (see e.g. Hillebrandt & Niemeyer 2000, for a review). However, the exact nature of the binary system is still under debate.

In the most commonly discussed scenario the CO WD accretes H from a non-degenerate companion star and explodes due to the onset of pycnonuclear reactions when the WD nears the Chandrasekhar-mass – the so called single-degenerate (SD) scenario (Whelan & Iben 1973; Nomoto 1982a). Alternatives are the double-degenerate (DD) scenario where two CO WDs merge due to gravitational wave emission (Iben & Tutukov 1984; Webbink 1984), or double detonations in sub-Chandrasekhar-mass He accreting CO WDs where the companion star can either be a He WD or He-burning star (Nomoto 1980, 1982b; Woosley et al. 1980, 1984).

The different progenitor scenarios leave characteristic im-

⋆ E-mail: markus.kromer@astro.su.se

© 2016 RAS

prints on the observational properties of SNe Ia, which have been used to obtain constraints on the progenitors (for a detailed review see Maoz et al. 2014). Unfortunately, the results of these analyses are not fully conclusive. On the one hand, the non-detection of companion stars in deep pre-explosion images of SN 2011fe and SN 2014J (e.g. Li et al. 2011; Kelly et al. 2014), the lack of X-ray and radio emission (e.g. Chomiuk et al. 2012; Margutti et al. 2012; Pérez-Torres et al. 2014), the absence of H features in the late-time spectra of SNe Ia (e.g. Shappee et al. 2013; Lundqvist et al. 2015; Maguire et al. 2016) and the non-detection of surviving companion stars in historic SN Ia remnants (e.g. Kerzendorf et al. 2009; Schaefer & Pagnotta 2012) favours DD progenitors. On the other hand, some SNe Ia show signs of circum-stellar material (e.g. Patat et al. 2007; Dilday et al. 2012), which are typically explained as the result of mass-transfer phases in SD progenitor systems (but see Shen et al. 2013). Furthermore, the chemical evolution of [Mn/Fe] requires that thermonuclear burning in near-Chandrasekhar mass WDs significantly contributed to the solar Fe abundance (see Seitenzahl et al. 2013a), which is most easily reconciled with some SNe Ia arising from SD progenitors.

Another smoking-gun signature of SD progenitors results from the collision of the SN ejecta with its non-degenerate companion star. Kasen (2010) has shown that this collision leads to reheating of parts of the ejecta and strong emission in the UV and blue bands for a few days after explosion. The strength and duration of the UV emission depend strongly on the binary separation and the viewing angle. Applying Kasen's models to results from binary population synthesis calculations, Liu et al. (2015) present the expected UV luminosity distribution for a variety of SD progenitor systems. Previous attempts at detecting ejecta-companion interactions in indvidual nearby SNe Ia (Nugent et al. 2011; Bloom et al. 2012; Brown et al. 2012; Goobar et al. 2015; Olling et al. 2015) and samples of SNe Ia from cosmological surveys (Hayden et al. 2010; Bianco et al. 2011) have been unsuccessful. Recently, however, the detections of an early ultraviolet flash in the peculiar SN Ia iPTF14atg (Cao et al. 2015) and an excess of blue light in the normal Type Ia SN 2012cg (Marion et al. 2016) have been interpreted as evidence for SD progenitors of these SNe.

Here, we investigate iPTF14atg in the context of state-of-the-art explosion models for different progenitor and explosion scenarios. The paper is organized as follows. In Section 2 we compile the observational properties of iPTF14atg and present a new late-time spectrum of the SN. In Section 3 we compare the observed spectra and light curves of iPTF14atg to synthetic observables from hydrodynamic explosion models for a SD progenitor and a WD merger. We discuss our findings in Section 4, before concluding in Section 5.

2 iPTF14atg

iPTF14atg was discovered on May 3.29, 2014 (UTC) when the intermediate Palomar Transient Factory (iPTF, Law et al. 2009) detected a new point source in the early-type galaxy IC 831 (Cao et al. 2015). The source was not present in observations on May 2.29, suggesting that the SN was caught very early with a likely explosion date between May 2.29 and 3.29. Here, we follow Cao et al. (2015) and assume May 3.0 for the time of explosion.

In the following weeks, the iPTF collaboration performed comprehensive observations of the new transient and obtained multi-band photometry with the Ultraviolet/Optical Telescope (UVOT) onboard the *Swift* space observatory and from various ground based observatories. They also followed the spectral evolution of iPTF14atg from early epochs to about 3 months after the explosion. The resulting observables and details on the data reduction are presented in Cao et al. (2015). For our study we have calibrated the spectral time sequence with respect to the PTF P48 R-band photometry.

From their observations, Cao et al. (2015) classified iPTF14atg as a slowly-evolving subluminous SN Ia with an absolute magnitude of -17.9 in the B band and a low expansion velocity. Comparing iPTF14atg to other subluminous SNe Ia they suggest it belongs to a class of objects similar to SN 2002es (Ganeshalingam et al. 2012). These objects show similar spectral features to 1991bg-like SNe, but significantly slower evolution and lower expansion velocities. Other known objects of this class include PTF10ops (Maguire et al. 2011) and SN 2010lp (Kromer et al. 2013b). A comparison to Type Iax SNe (Foley et al. 2013) was also attempted but found to be less favourable.

The extensive data set of iPTF14atg clearly makes it the best observed member of the 2002es-like class. What makes it really special is a high flux in the *Swift* UV bands at the earliest epoch (4 d past explosion), which is followed by a steep decline lasting about 1 d before the UV flux rises again (fig. 1 of Cao et al. 2015). Such an initial UV pulse has not been observed in any other SN Ia before. Given that no other 2002es-like SNe have been observed at comparably early epochs, it is not clear whether this is a unique feature of iPTF14atg or typical for this class of objects.

Cao et al. (2015) discuss several possibilities to explain the initial UV pulse, including a layer of radioactive isotopes in the outer ejecta, shock interaction with the circum-stellar medium and interactions between the SN ejecta and a non-degenerate companion star. They conclude that companion interaction is the only viable scenario, claiming a SD progenitor for iPTF14atg.

2.1 Nebular spectrum

We obtained an optical spectrum of iPTF14atg on December 21, 2014 (corresponding to 232 d past explosion) with the Deep Imaging Multi-Object Spectrograph (DEIMOS; Faber et al. 2003) mounted on the 10 m Keck II telescope. The instrument was set up with the 600 lines mm^{-1} grating, providing spectral coverage over the region $\lambda = 4500$–9500 Å with a spectral resolution of 3.5 Å. The spectrum was optimally extracted (Horne 1986), and the rectification and sky subtraction were performed following the procedure described by Kelson (2003). The slit was oriented at the parallactic angle to minimize losses due to atmospheric dispersion (Filippenko 1982).

This late-time spectrum, presented in Figure 1, clearly shows forbidden emission lines of Fe, which are the hallmark feature of SNe Ia in the nebular phase. Specifically, we find pseudo-continuous [Fe II] emission blueward of $\sim$5500 Å and a strong emission feature at 7000-7500 Å, which is typically attributed to [Fe II] $\lambda 7155$ and [Ca II] $\lambda\lambda 7291, 7323$. This is very similar to the behaviour of subluminous 1991bg-like SNe Ia (Mazzali et al. 1997; Mazzali & Hachinger 2012).

In addition, iPTF14atg shows a pronounced emission feature at $\sim$6300 Å, which is not observed in 1991bg-like SNe Ia. However, a similar feature was observed in the 2002es-like SN 2010lp by Taubenberger et al. (2013), thus corroborating the classification of iPTF14atg as a 2002es-like SN by Cao et al. (2015). The nature of this 6300 Å feature has not yet been investigated with detailed radiative transfer models. Taubenberger et al. (2013) attribute it to

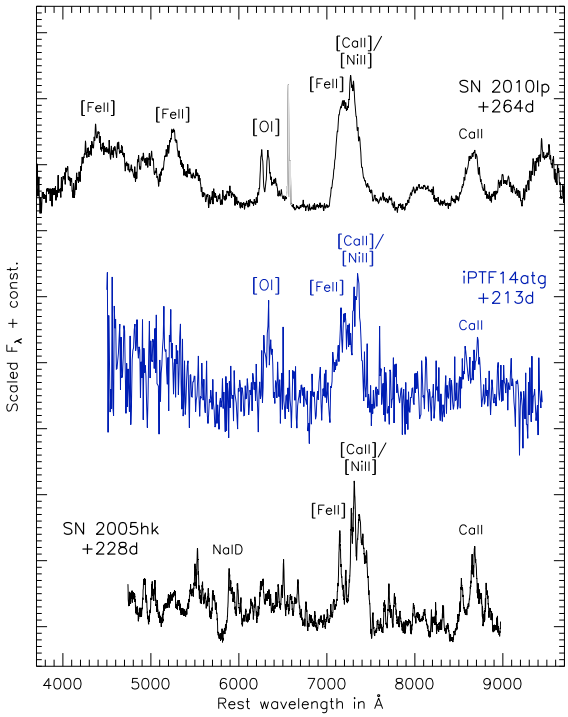

Figure 1. The nebular Keck-DEIMOS spectrum of iPTF14atg taken at 213 d past B-band maximum (blue, the spectrum was re-binned to a wavelength resolution of 8 Å to increase the signal-to-noise ratio). Note the emission feature at 6300 Å. For comparison late-time spectra of the 2002es-like SN 2010lp (Taubenberger et al. 2013) and the Type Iax SN 2005hk (Sahu et al. 2008) are shown at +264 d and +228 d, respectively. Narrow Hα emission in the spectrum of SN 2010lp, originating from a nearby H II region, has been greyed out to highlight the intrinsic SN features.

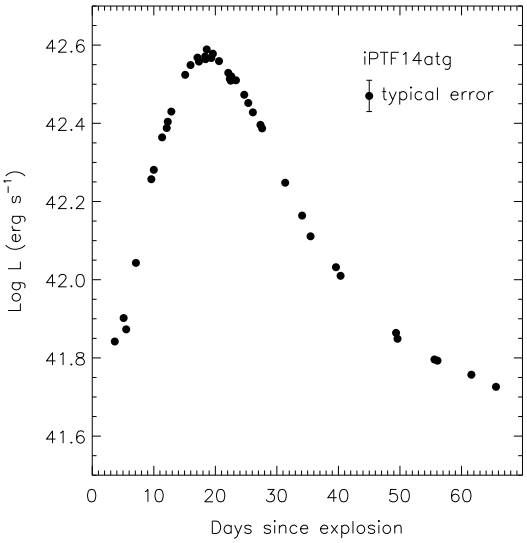

Figure 2. Pseudo-bolometric light curve of iPTF14atg.

2.2 Bolometric light curve

Figure 2 shows a pseudo-bolometric light curve of iPTF14atg, which we have constructed from the observed broad-band photometry ($uvw2, uvm2, uvw1, U, B, g, V, r, i$), adopting a distance modulus of 34.85 ± 0.1 mag according to NED[1] and a Galactic extinction of $A_B^{\rm gal} = 0.03$ mag along the line of sight towards IC 831. Looking at the Na I D doublet in the spectra of iPTF14atg, the host extinction is negligible and we adopt $A_B^{\rm host} = 0.00 \pm 0.02$ mag. Errors on the bolometric flux are dominated by the uncertainties on the distance modulus and the extinction, and are indicated by a typical error bar in Figure 2. For the peak luminosity of iPTF14atg we find a value of $\log\ L_{\rm peak} = 42.58 \pm 0.04$ ($\log {\rm erg\,s^{-1}}$).

[O I] $\lambda\lambda 6300, 6364$ emission in analogy to the nebular spectra of Type Ib/c SNe (e.g. Maeda et al. 2008; Taubenberger et al. 2009).

This would require a significant fraction of O in the central parts of the explosion ejecta. While pure detonations and delayed detonations of Chandrasekhar-mass WDs do not leave sufficient O in the central ejecta (e.g. Seitenzahl et al. 2013b), turbulent burning in Chandrasekhar-mass deflagrations distributes O all over the ejecta (e.g. Röpke et al. 2007; Ma et al. 2013). It has been shown that such deflagration models indeed lead to [O I] emission at late times (Kozma et al. 2005). However, due to the mixing, these features are fairly broad. Therefore, Taubenberger et al. (2013) discard this model for the narrow [O I] features seen in SN 2010lp. Instead, they favour a violent merger like that by Pakmor et al. (2012b), where unburned O from the secondary WD is present at low velocities in the central ejecta but no strong mixing.

A connection of iPTF14atg to Type Iax SNe, which was discussed but already discarded by Cao et al. (2015), seems also unlikely from a comparison of the late-time spectra. The prototypical Type Iax SN 2005hk does not show an emission feature at ∼6300 Å. Instead, late-time spectra of Type Iax SNe are still dominated by low-velocity P-Cygni profiles of permitted Fe lines (Jha et al. 2006). Given the poor S/N of our late-time spectrum we can unfortunately not test this for iPTF14atg.

3 MODELS

3.1 Chandrasekhar-mass models

Owing to the early-time UV pulse, Cao et al. (2015) favour a SD origin for iPTF14atg. The most common explosion scenario for the SD progenitor channel, is an explosion at the Chandrasekhar-mass (e.g. Wang & Han 2012). This scenario comes in several flavours depending on the mode of flame propagation. A prompt detonation produces almost pure ^{56}Ni ejecta (Arnett 1969) which is not consistent with the observed properties of SNe Ia (e.g. Mazzali et al. 2007).

Instead, the delayed detonation scenario, where the flame starts as a subsonic deflagration and transitions to a supersonic detonation at a later stage (Khokhlov 1991), has become the standard model to produce SNe Ia in the Chandrasekhar-mass scenario (e.g. Kasen et al. 2009). Sim et al. (2013) have recently explored the observable parameter space of delayed detonations from a sample of state-of-the-art 3D explosion models (Seitenzahl et al. 2013b) and find peak bolometric luminosities in the range $\log\ L_{\rm peak} =$

[1] The NED estimate is based on a cosmology with $H_0 = 73\,{\rm km\,s^{-1}\,Mpc^{-1}}$, $\Omega_{\rm m} = 0.27$ and $\Omega_\Lambda = 0.73$, and a redshift of $z = 0.021405$

$42.80 - 43.31$ ($\log \mathrm{erg\,s^{-1}}$). Given the wide range of ignition configurations covered by these models, it seems unlikely that a delayed detonation can account for iPTF14atg ($\log\ L_{\rm peak} = 42.58 \pm 0.04$). Moreover, the synthetic spectra of the models do not match iPTF14atg: line expansion velocities are generally too large and absorption features are too strong, particularly before peak.

In the Chandrasekhar-mass scenario, weaker (and fainter) explosions can be obtained from pure deflagrations. Fink et al. (2014) present hydrodynamic explosion simulations and synthetic observables for a set of 3D deflagration models in Chandrasekhar-mass CO WDs, covering a wide range of ignition strengths. iPTF14atg lies well in the range of peak bolometric luminosities $\log\ L_{\rm peak} = 42.06 - 42.86$ ($\log \mathrm{erg\,s^{-1}}$) covered by these deflagrations models. The closest match in terms of peak bolometric luminosity is provided by model N5def ($\log\ L_{\rm peak} = 42.59$). With five ignition kernels in a small solid angle, N5def burns only a small fraction of the initial WD (see figure 2 of Kromer et al. 2013a). Since the nuclear energy release is less than the binding energy of the initial WD, only $0.37\,\mathrm{M_\odot}$ of material are ejected in the explosion (kinetic energy 1.34×10^{50} erg) and a bound remnant of $\sim 1.03\,\mathrm{M_\odot}$ is left behind. Owing to the turbulent evolution of the deflagration flame, the ejecta are well mixed with a composition predominantly of iron-group elements (IGEs, $0.222\,\mathrm{M_\odot}$), unburned O ($0.060\,\mathrm{M_\odot}$), C ($0.043\,\mathrm{M_\odot}$) and intermediate-mass elements (IMEs, $0.042\,\mathrm{M_\odot}$). With a ^{56}Ni yield of $0.158\,\mathrm{M_\odot}$ the ejecta of N5def give rise to a faint transient in good agreement to SN 2005hk, a proto-typical SN Iax (see Kromer et al. 2013a for a detailed discussion of the properties and synthetic observables of N5def). Here, we explore whether an explosion similar to N5def can explain the observable properties of iPTF14atg.

Figure 3 shows synthetic light curves of model N5def along 100 different viewing angles in various photometric bands. The diversity with viewing angle is strongest in the UV bands and decreases at longer wavelengths. Overall the viewing angle sensitivity is relatively modest since the turbulent deflagration produces well-mixed ejecta. For comparison we overplot the observed photometry of iPTF14atg as reported by Cao et al. (2015). Although N5def provides a good match regarding the peak brightness of iPTF14atg, the model's time evolution is significantly too fast. In the B band, for example, the model peaks between 10.4 and 12.2 d, depending on viewing angle, while iPTF14atg peaked at 19.2 d. This indicates that the diffusion time is too short and the ejecta mass of N5def is too low compared to iPTF14atg.

Similar problems can be observed in the spectral evolution of the N5def model. Figure 4 shows synthetic spectra for 100 different viewing angles between 8 and 33.6 d past explosion. As for the light curves, the time evolution of the spectral time series of N5def is significantly too fast compared to iPTF14atg. Moreover, there are a number of prominent discrepancies between the spectral features of the model and the data. At all epochs, the model shows two prominent emission features at $\sim$ 4500 and 5000 Å which are not observed in iPTF14atg. Starting at 18.3 d past explosion, the model predicts too low flux levels blueward of $\sim$ 4500 Å indicating too much line blocking by the large fraction of IGEs in the model ejecta.

More energetic deflagration models burn the full WD and lead to larger ejecta masses (Fink et al. 2014). However, at the same time they also produce significantly larger amounts of ^{56}Ni in the ejecta, leading to peak bolometric luminosities too bright for iPTF14atg [$\log\ L_{\rm peak} = 42.77 - 42.86$ ($\log \mathrm{erg\,s^{-1}}$) for the models of Fink et al. 2014] and a mismatch in the spectral evolution.

In summary, from our comparison between iPTF14atg and a

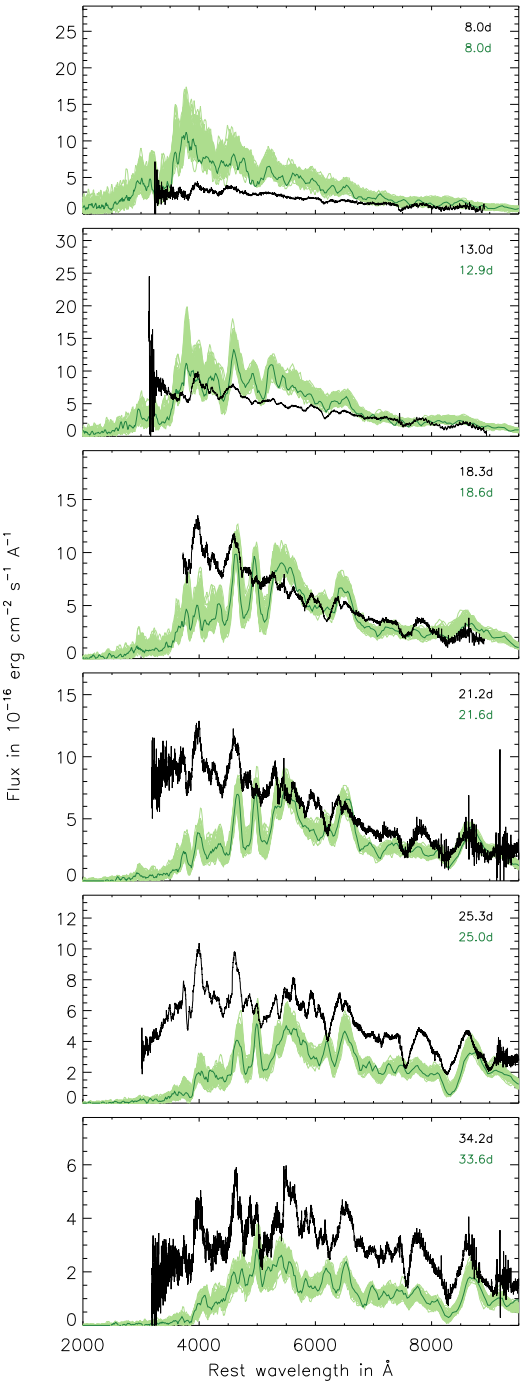

Figure 4. Snapshots of the spectral evolution of N5def for 6 epochs between 8 and 33.6 d past explosion (the exact epochs are indicated in the individual panels). The dark green line shows spectra for a selected viewing angle (fixed for all epochs). To indicate the viewing angle diversity, we also show the spectra from 100 lines of sight (light green), which are equally distributed over the full solid angle. Observed spectra of iPTF14atg, which have been de-redshifted and de-reddened with $E(B-V) = 0.011$ to account for the Galactic extinction towards IC 831, are shown in black for comparable epochs.

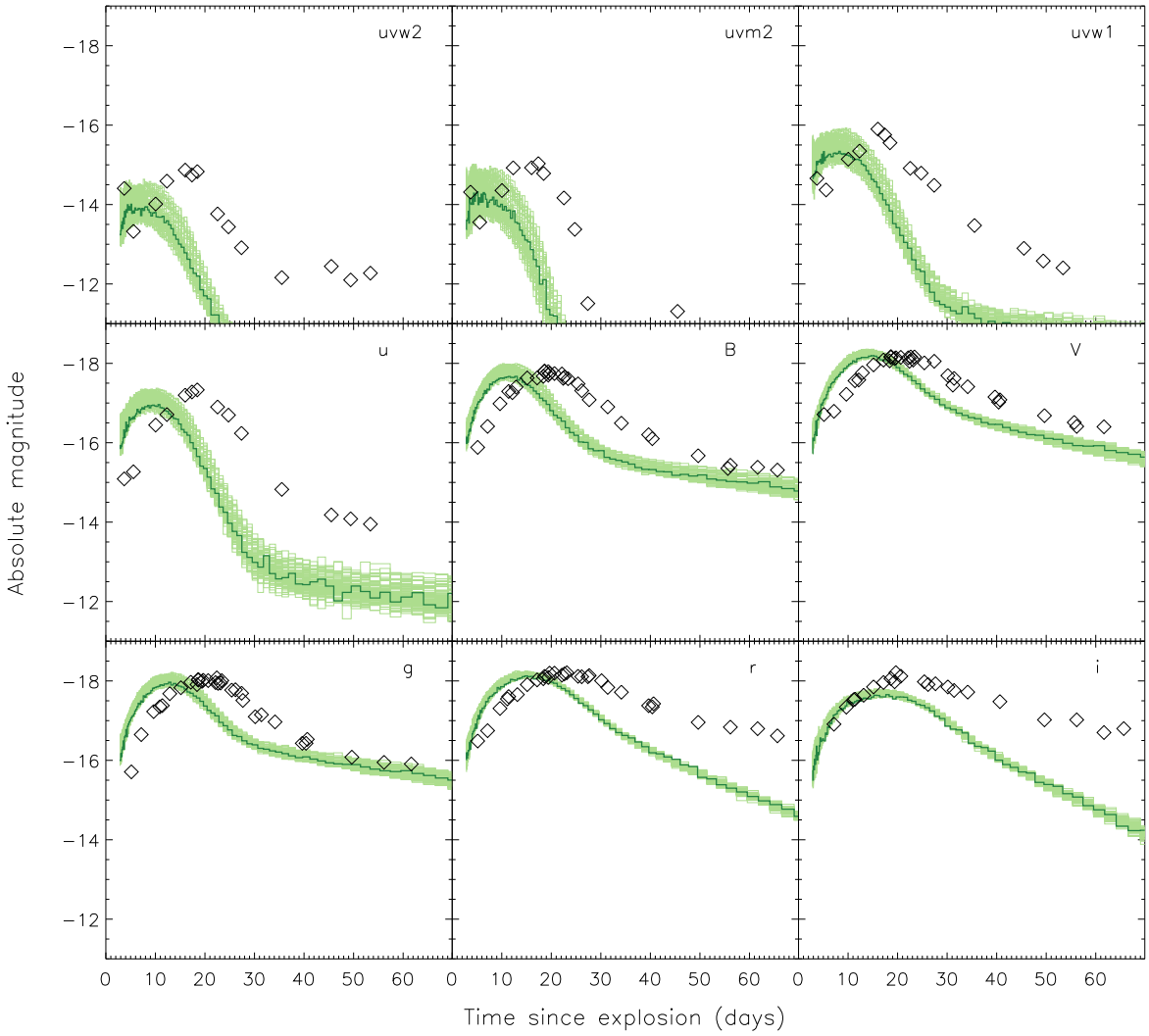

Figure 3. Broad-band synthetic light curves of N5def in various bands: *Swift* UVOT $uvw2$, $uvm2$, $uvw1$, u, Bessell B, V and SDSS g, r, i (from top left to bottom right, respectively). UVOT and SDSS magnitudes are in the AB system, Bessell magnitudes in the Vega system. The region coloured in light green indicates the viewing angle diversity, while the dark green line shows a particular viewing angle (the same viewing angle has been selected for the different photometric bands and the spectral time series of the N5def model, presented in Figure 4). The observed photometry of iPTF14atg is shown as black diamonds, assuming May 3.0 as the time of explosion (Cao et al. 2015), a distance modulus of 34.85 mag for IC 831 and de-reddened for a Galactic extinction of $E(B-V) = 0.11$.

wide variation of Chandrasekhar-mass explosion models (Sim et al. 2013; Fink et al. 2014), we find it unlikely that a Chandrasekhar-mass explosion can explain the observational properties of iPTF14atg. Thus, we explore alternative models in the following.

3.2 Solar-metallicity merger model

Given the likely classification of iPTF14atg as a 2002es-like SN Ia, violent mergers in WD binaries could be promising candidates to explain the observed properties of iPTF14atg. For SN 2010lp, another 2002es-like SN Ia, Kromer et al. (2013b) reported remarkably good agreement with the synthetic observables of a violent merger model.

In their particular model, Kromer et al. (2013b) use the smoothed-particle-hydrodynamics (SPH) code GADGET (Springel 2005; Pakmor et al. 2012a) to simulate the final inspiral of two CO WDs with 0.90 and 0.76 $\mathrm{M}_\odot$, respectively (cf. figure 1 of Kromer et al. 2013b). Rapid accretion of material from the secondary (less massive) WD onto the primary causes compressional heating sufficient to ignite thermonuclear burning of C in the simulation. Assuming that a detonation forms in the hottest cell, Kromer et al. (2013b) simulate the explosion dynamics with the grid-based LEAFS code (Reinecke et al. 2002) and find that the detonation completely disrupts the merged object within ~ 2 s, ejecting $\sim 1.6\,\mathrm{M}_\odot$[2] that stream freely at ~ 100 s after the detonation (asymptotic kinetic energy $1.1. \times 10^{51}$ erg). Since the detonation front propagates faster in the high-density material of the primary WD, explosion ashes from the primary can partially engulf the secondary before it is disrupted. This leads to complex structures with pronounced large-scale asymmetries and unburned

[2] When mapping the initial SPH simulation to the LEAFS grid some mass is lost, since a number of SPH particles lie outside the simulated grid domain.

O (from the secondary WD) in the central parts of the ejecta (cf. figure 2 in Kromer et al. 2013b). The detailed nucleosynthetic yields of the explosive burning are derived in a post-processing step with a 384-isotope nuclear network (Travaglio et al. 2004), yielding a ^{56}Ni mass of $0.18\,\mathrm{M}_{\odot}$. To facilitate a comparison of the explosion model to SN light curves and spectra, Kromer et al. (2013b) obtain synthetic observables with the multi-dimensional Monte Carlo radiative transfer code ARTIS (Kromer & Sim 2009; Sim et al. 2007). For more details on the simulation setup and results see Kromer et al. (2013b).

Here, we take the model of Kromer et al. (2013b) and compare it to the observed properties of iPTF14atg. Figure 5 shows synthetic light curves of the model along 100 different viewing angles in various photometric bands. Owing to the large-scale asymmetries in the merger ejecta, the light curves show a prominent viewing angle sensitivity. After 10 d past explosion, the merger model matches iPTF14atg reasonably well in V and redder bands. At earlier epochs and in the bluer bands the model shows a pronounced flux deficit compared to iPTF14atg.

The same behaviour can be seen for the spectral evolution (Figure 6, left panel). At 8 d the model flux is significantly lower than the observed spectrum of iPTF14atg. From 12.9 to 33.6 d the overall spectral energy distribution (SED) of the model is in good agreement with the observed SED of iPTF14atg. Small differences in the SED become visible where the observed spectra extend to the UV, indicating a deficit of UV photons in the model.

Taking a closer look, the merger spectra also reproduce the key spectral features of iPTF14atg. A striking difference, however, is visible for the Ti II dominated region between 4000 and 4400 Å which shows a strong absorption trough in the model spectra that is not present in iPTF14atg. A similar behaviour can be observed for the Ca II features. Both the H&K doublet and the NIR triplet are far too strong in the model, particularly at early epochs. The latter problem might be related to the composition of the progenitor WDs in the model of Kromer et al. (2013b). Assuming WDs from main-sequence progenitors with solar metallicity ($Z_{\odot}$), Kromer et al. (2013b) adopt an initial WD composition of 50% O and 48.29% C (by mass). The remaining 1.71% are distributed according to the solar abundances of Asplund et al. (2009) for all elements but H and He (primordial C, N, and O were converted to ^{22}Ne to account for core He-burning). This introduces a significant contribution of Ca and Ti in the unburned outer ejecta, which may be responsible for the deep and broad Ca and Ti features.

3.3 Reducing the metallicity of the merger model

For a low-metallicity progenitor system the unburned outer layers will have lower Ca and IGE contents. This might help to alleviate some of the shortcomings discussed in the previous paragraph. To explore the influence of this effect, we have repeated the postprocessing and radiative transfer simulations for a lower metallicity progenitor system of our 0.90+$0.76\,\mathrm{M}_{\odot}$ merger. Specifically, we have assumed $Z = 0.01Z_{\odot}$ for the progenitor WDs. The spectral time series of this new calculation is shown in the right hand panel of Figure 6. Compared to the original model, the Ca features are significantly weaker, which brings the model in better agreement with the observed features of iPTF14atg. Remarkably, the new model also agrees almost perfectly with iPTF14atg in the Ti II dominated region between 4000 and 4400Å. The outer ejecta layers of our modified merger model contain much less Ti than those of the original model of Kromer et al. (2013b) that started from solar metallicity progenitors. Consequently, the Ti II absorption is significantly lower in our new model, leading to much better agreement with iPTF14atg.

Moreover, we find a notably increased UV flux for the new model while the flux level between 4500 and 7000 Å, is slightly reduced. This improves the agreement of the model SED with the data. In the original model the unburned outer ejecta layers are polluted with IGEs in solar composition. This leads to a strong suppression of UV flux by line blocking which is then redistributed to optical wavelengths, where the radiation escapes from the ejecta. In the new model the IGE content of the unburned layers is reduced by a factor 100, leading to significantly less line blocking. As a consequence the new model also evolves slightly faster. We find a B-band peak time of 19.8 d which is in good agreement with the rise time of 19.2 d of iPTF14atg [the original merger model of Kromer et al. (2013b) has a rise time of 21.3 d, for comparison]. This also leads to an increased flux at early epochs and brings the model in closer agreement with the 8 d spectrum, although the model flux is still too low for the majority of viewing angles.

Figure 7 shows synthetic light curves for the new model. After about 10 d past explosion the agreement between the new model and iPTF14atg in the optical bands is excellent. In the *Swift* UV filters ($uvw2$,$uvm2$,$uvw1$), the reduced line blocking leads to significantly increased peak flux and much better agreement with iPTF14atg. While the original model showed a clear flux deficit in these bands (compared to the data), some lines-of-sight of the new model have a UV flux level comparable to iPTF14atg. In fact, the majority of viewing angles has higher UV flux than iPTF14atg. This leaves room for a progenitor system with sub-solar metallicity for iPTF14atg. Constraining the chemical composition of the progenitor system more precisely, would require a large set of models for different metallicities. But even then the large viewing-angle sensitivity in the UV will make it difficult to determine an exact value for the progenitor composition. In addition, other parameters like the initial masses of the WDs or the time of ignition will also affect the observational display, making the potential parameter space even larger. We thus do not aim to obtain a perfect fit with our new $Z = 0.01Z_{\odot}$ model, but stress that a violent merger with low progenitor metallicity can provide an excellent match to iPTF14atg.

We also note that our merger model contains a significant fraction of O in the central parts of the ejecta, which originates from the secondary WD and is at too low initial density to be burned within the explosion (cf. figure 2 in Kromer et al. 2013b). This could lead to [O I] emission as observed in iPTF14atg, given that the excitation and ionization conditions are appropriate. Unfortunately, we can currently not simulate this directly, since our 3D radiative transfer code ARTIS does not account for the necessary non-thermal excitation and ionization processes. One-dimensional models with a more sophisticated excitation treatment are only of limited use. Mapping the highly asymmetric ejecta of our merger model to 1D leads to artificial mixing of chemical species, which introduces a multitude of additional complications. A detailed investigation of the late-time spectrum must therefore be postponed to future work.

4 DISCUSSION

Our models indicate that it will be difficult to explain iPTF14atg in the context of Chandrasekhar-mass explosions. Lowering the metallicity of the progenitor system will not significantly affect the observables in this case, since burning ashes are mixed to the outer ejecta during the turbulent deflagration phase (e.g. Seitenzahl et al.

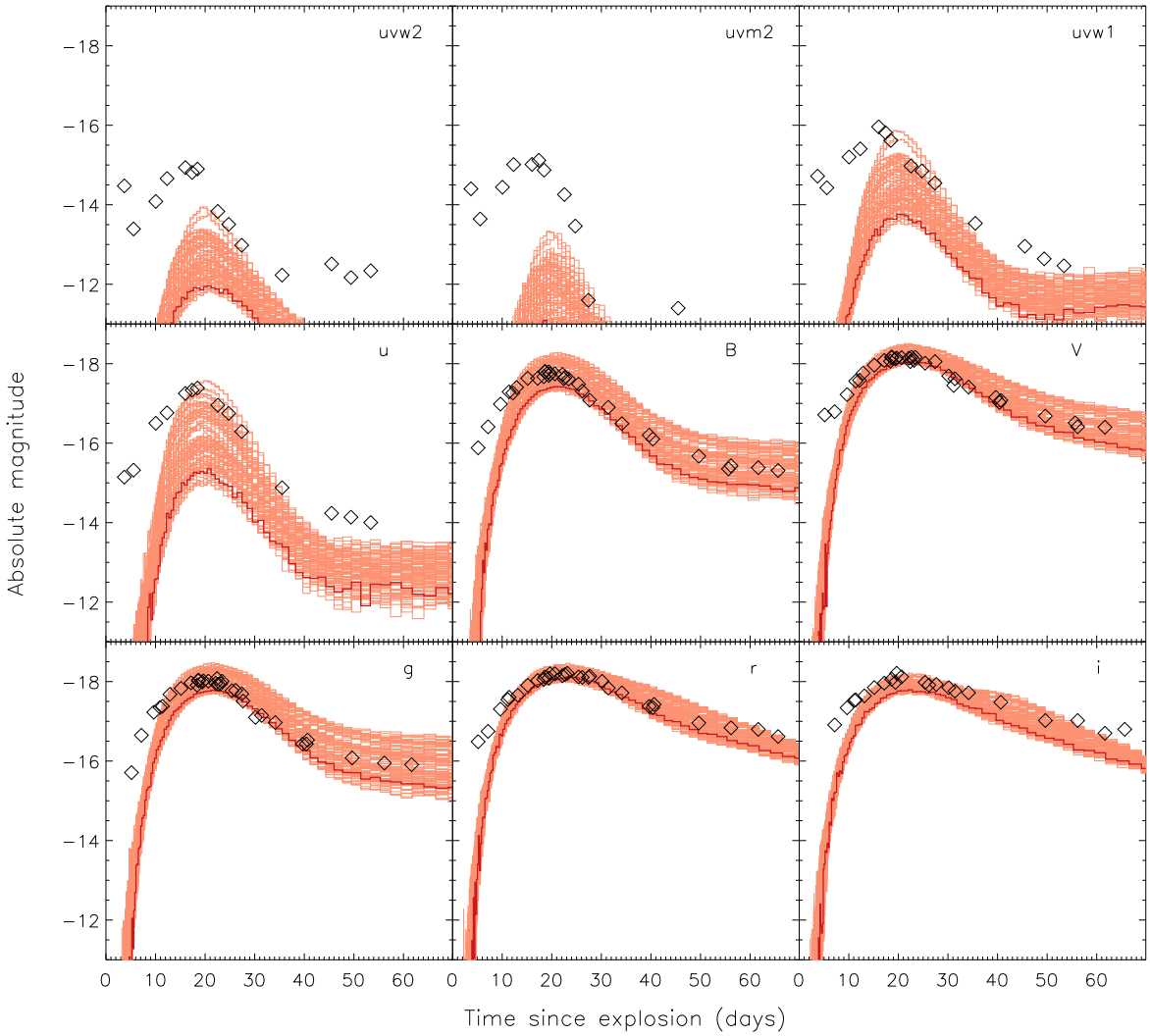

Figure 5. Broad-band synthetic light curves of the violent merger of two CO WDs (0.90+$0.76\,\mathrm{M}_{\odot}$, Kromer et al. 2013b) in various bands: *Swift* UVOT $uvw2$, $uvm2$, $uvw1$, u, Bessell B, V and SDSS g, r, i (from top left to bottom right, respectively). UVOT and SDSS magnitudes are in the AB system, Bessell magnitudes in the Vega system. The region coloured in light red indicates the viewing angle diversity, while the dark red line shows a particular viewing angle [the same viewing angle has been selected for the different photometric bands and the spectral time series of the violent merger of Kromer et al. (2013b), presented in the left panel of Figure 6]. The observed photometry of iPTF14atg is shown as black diamonds, assuming May 3.0 as the time of explosion (Cao et al. 2015), a distance modulus of 34.85 mag for IC 831 and correcting for Galactic reddening.

2013b). Consequently, the IGE mass fraction is well above the solar composition in most of the ejecta (for pure deflagration models, like N5def presented in Section 3.1, over the full velocity range of the ejecta). Thus, an 0.1% contribution of progenitor IGEs for a model with solar metallicity does not have a strong impact on the observables of Chandrasekhar-mass explosions. This is only the case, if there are large parts of the ejecta that do not contain freshly synthesized IGEs like in our merger model.

An alternative SD progenitor option could be a double detonation in a He-accreting sub-Chandrasekhar-mass WD. If accreting from a non-degenerate He star donor, such a system belongs to the SD progenitor class. A number of simulations have shown that double detonations can lead to faint SNe Ia (e.g. Höflich & Khokhlov 1996; Fink et al. 2010; Woosley et al. 2011). However, there are several potential problems. (i) It has been predicted that the ashes of the first detonation in the He shell should leave characteristic imprints around maximum light (Kromer et al. 2010), which are not observed in the case of iPTF14atg. (ii) Having an explosion below the Chandrasekhar-mass will lead to low ejecta mass and short diffusion time – in contrast to the slow evolution observed for iPTF14atg. In fact, sub-Chandrasekhar double detonations have been proposed to explain the rapidly evolving subluminous 1991bg-like SNe Ia, owing to their fast light curve evolution (Stritzinger et al. 2006; Scalzo et al. 2014). (iii) With a He-accreting double detonation model it will be difficult to explain the 6300 Å feature in the late-time spectrum. [O I] emission seems impossible since no O will be left in the central ejecta. (iv) In addition, for the case of a double detonation in a SD progenitor system, i.e. a sub-Chandrasekhar-mass WD accreting from a non-degenerate He star donor, the theoretical delay-time distribution is strongly peaked at short times (< 500 Myr, Ruiter et al. 2011). This makes such systems unlikely progenitors for 2002es-like SNe, which have been observed preferentially (but not exclusively) in massive early-type host galaxies (White et al. 2015).

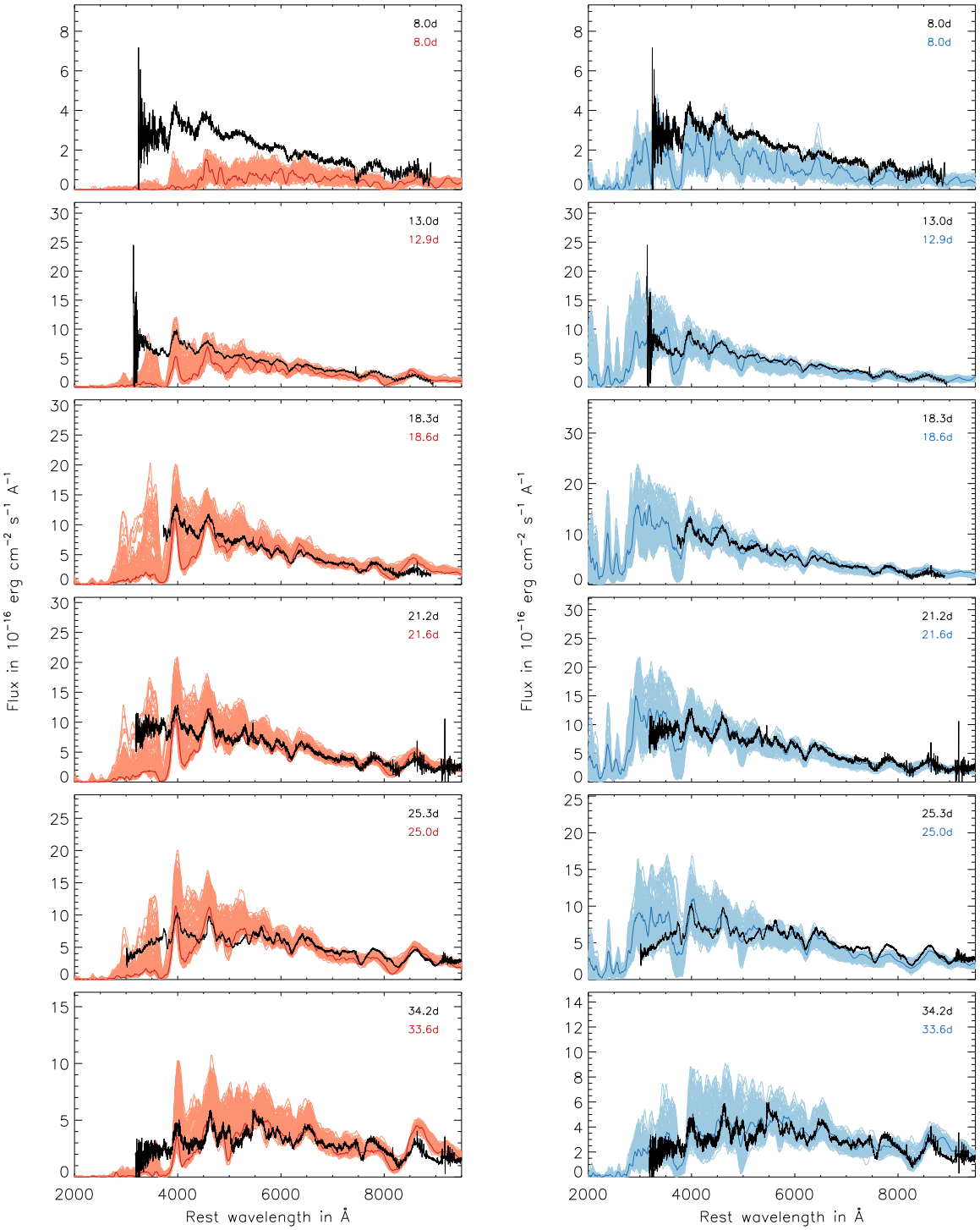

Figure 6. *Left:* Synthetic spectra for the violent merger model of Kromer et al. (2013b) where the progenitor WDs have been admixed with metals heavier than C and O in solar composition. The dark red line shows spectra for a selected viewing angle (fixed for all epochs). To indicate the viewing angle diversity, we also show the spectra from 100 lines of sight (light red), which are equally distributed over the full solid angle. Observed spectra of iPTF14atg (de-redshifted and de-reddened) are shown in black for comparable epochs. *Right (in blue colour scheme):* Same as left hand panel but for a modified merger model from a progenitor system with reduced metallicity ($Z = 0.01 Z_{\odot}$).

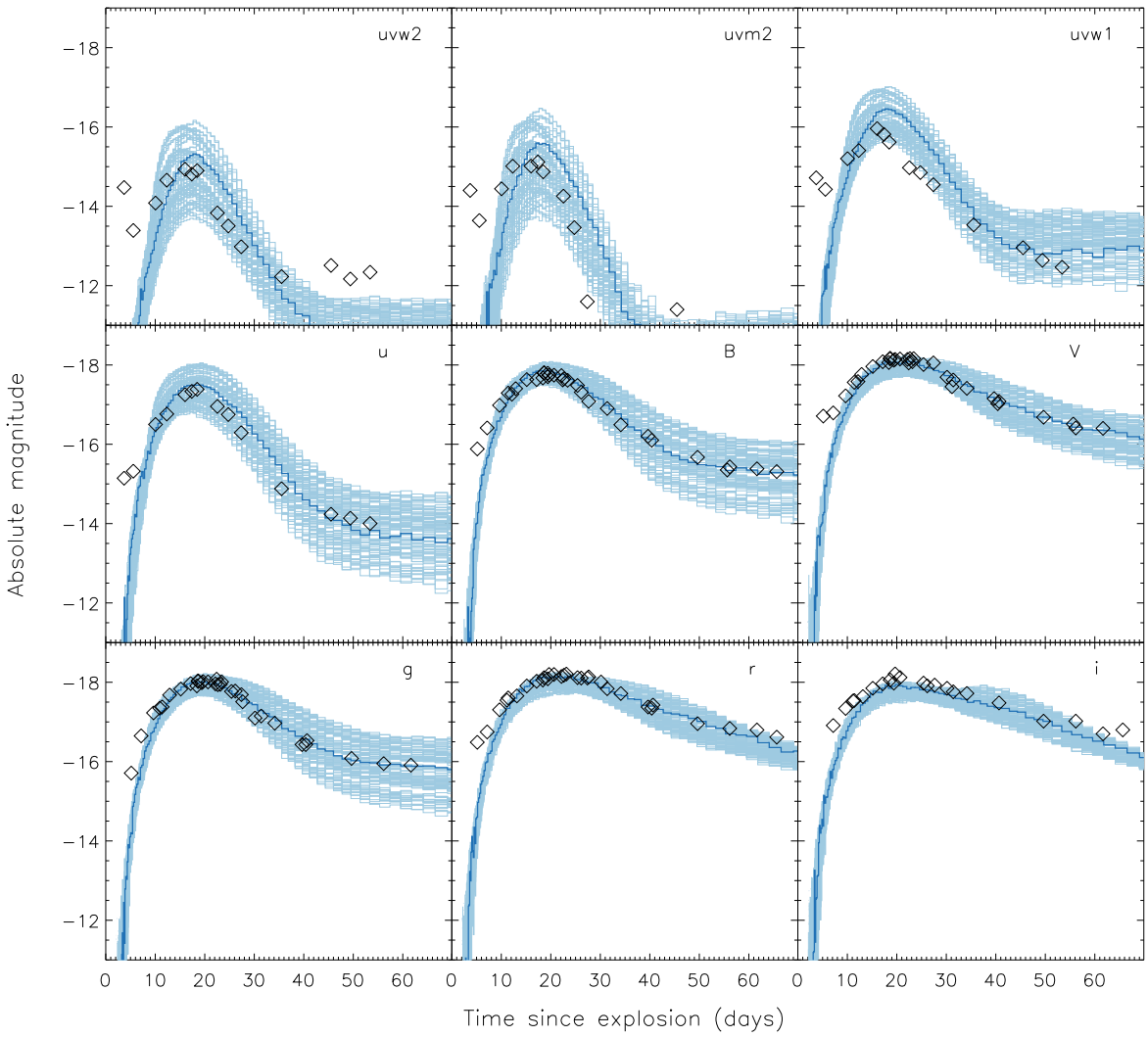

Figure 7. Broad-band synthetic light curves of our new $0.90{+}0.76\,\mathrm{M}_\odot$ violent merger model with $Z = 0.01Z_\odot$: *Swift* UVOT $uvw2$, $uvm2$, $uvw1$, u, Bessell B, V and SDSS g, r, i (from top left to bottom right, respectively). UVOT and SDSS magnitudes are in the AB system, Bessell magnitudes in the Vega system. The region coloured in light blue indicates the viewing angle diversity, while the dark blue line shows a particular viewing angle (the same viewing angle has been selected for the different photometric bands and the spectral time series of our $Z = 0.01Z_\odot$ violent merger, presented in the right panel of Figure 6). The observed photometry of iPTF14atg is shown as black diamonds, assuming May 3.0 as the time of explosion (Cao et al. 2015), a distance modulus of 34.85 mag for IC 831 and correcting for Galactic reddening.

Taking all together, from the models we have at hand a SD progenitor of iPTF14atg seems unlikely. In contrast, the merger model presented in the previous section shows excellent agreement with the observed properties of iPTF14atg after about 10 d past explosion. There are, however, some discrepancies at the earliest epochs. In particular, our model cannot naturally explain the early UV pulse in the *Swift* observations (compare e.g. Figure 7). In the following, we discuss possibilities how to account for the early-time UV pulse in a merger scenario.

4.1 CSM interaction

In some core-collapse explosions of massive stars a similar behaviour to the early light curve of iPTF14atg is observed (e.g. Gezari et al. 2008). This is attributed to cooling of shock heated ejecta immediately after the shock breakout (Rabinak & Waxman 2011). For exploding WDs the radius is so small that the time scales for shock breakout are very short and the additional luminosity is too faint to be detected (e.g. Piro et al. 2010; Rabinak et al. 2012). However, it has been argued that shock interaction with an extended circum-stellar medium (CSM), which happens on longer time scales, could lead to additional early-time optical/UV emission (e.g. Raskin & Kasen 2013; Levanon et al. 2015).

Cao et al. (2015) have ruled out such a scenario for iPTF14atg. However, they have only investigated the special case of an extended optically thin CSM in a spherically symmetric configuration. The potential parameter space for the CSM configuration of DD mergers is however larger and a spherically symmetric configuration seems highly unlikely for systems that explode on the dynamical or viscous time scale.

Raskin & Kasen (2013) discuss the signatures of CSM interaction in WD mergers for a variety of CSM configurations with a focus on tidal tails (see also Levanon et al. 2015). Depending on the lag time between the time of the tidal tail ejection and the time

when the merged system explodes, they find a wide range of observables. For lag times on the order of the viscous time scale of the merger, the CSM is not very extended ($r \lesssim 10^{13}$ cm). For this case Raskin & Kasen (2013) predict a soft ($\sim$100 eV) shock breakout signal from tidal tail interaction that lasts for a few minutes and is followed by bright optical/UV cooling emission ($L_{\rm bol} = 10^{42} - 10^{43}\,{\rm erg\,s^{-1}}$). This is fairly similar to the early-time UV luminosity ($L_{\rm UV} = 3 \times 10^{41}\,{\rm erg\,s^{-1}}$) that Cao et al. (2015) reported for iPTF14atg. However, Raskin & Kasen (2013) also note that, owing to the low mass of the tidal tails, the duration of the optical/UV cooling emission should be fairly short. They estimate a duration of about half a day. This is too short to explain the initial UV pulse of iPTF14atg, which lasted for several days.

Sophisticated radiation hydrodynamics simulations, exploring a wider range of CSM configurations for merger models from various initial parameters, will be required to investigate the observable display of the CSM interaction scenario in more detail and evaluate its potential to explain the early-time luminosity of iPTF14atg. However, it is interesting to note that Piro & Morozova (2015) have recently shown that CSM interaction can – at least in the optical – lead to similar effects in the early-time light curves as for the case of interactions between the SN ejecta and a non-degenerate companion star (Kasen 2010).

4.2 Surface radioactivity

Another possibility to explain the early-time UV pulse could be radioactive material close to the ejecta surface. This is characteristic for double detonations in He accreting systems (e.g. Fink et al. 2010; Woosley & Kasen 2011). Recently, high resolution simulations of WD mergers by Pakmor et al. (2013) and Tanikawa et al. (2015) have shown that even a thin He layer, which is expected on most CO WDs according to stellar evolution calculations, is sufficient to lead to a He shell detonation (the resolution of the merger model presented here is not high enough to resolve such a He layer). Both Pakmor et al. (2013) and Tanikawa et al. (2015) find that this initial He detonation can trigger a secondary detonation in the more massive component of the merger by converging shock fronts (He-ignited violent merger scenario). In this case the observational display of the explosion would be rather similar to a sub-Chandrasekhar-mass double detonation with all the problems discussed above.

However, Tanikawa et al. (2015) note that the triggering of the secondary detonation could also fail e.g. due to inhomogeneities in the He shell or instabilities in the burning. In this case the system survives the He shell detonation and a "classical" carbon-ignited violent merger explosion might occur at a later epoch, given that sufficiently high temperatures and densities are reached. The observational display would then be very similar to a "classical" carbon-ignited violent merger explosion as presented in this paper, with the additional complication of ashes from the initial He shell detonation at the surface of the ejecta.

Cao et al. (2015) have shown that a shell of 0.01 $\rm M_\odot$ of ^{56}Ni would be required to explain the early time UV flux of iPTF14atg, which is comparable to theoretical predictions in double detonation models (e.g. Fink et al. 2010; Woosley & Kasen 2011). However, Cao et al. (2015) disfavour surface radioactivity as the source for the early time UV flux. They argue that flux redistribution to the optical/NIR would suppress the UV flux (Kromer et al. 2010). However, the discussion in Kromer et al. (2010) refers to effects around the peak of the optical light curves. At these epochs iron-group elements in the He shell ashes act mainly as an opacity source and are very efficient in redistributing blue photons that originate from ^{56}Ni in the centre of the ejecta (ashes from the core detonation) to redder wavelengths when propagating towards the surface of the ejecta. At early times the situation is different. There, the densities are still high so that local deposition of radioactive energy in the shell material dominates, thereby heating the shell and leading to a strong UV flux.

As outlined above, the critical point for a scenario with a He surface detonation is to have sufficient radioactive material in the outer layers to explain the early UV flash, but at the same time not too much iron-group elements to avoid strong flux redistribution at optical peak. In double detonations with massive He shells that are ignited by a thermal instability this seems difficult, since the shell masses are fairly large (e.g. Kromer et al. 2010; Woosley & Kasen 2011). However, in mergers it is possible to ignite much smaller He shell masses dynamically (e.g. Guillochon et al. 2010; Pakmor et al. 2013). Whether such models produce enough surface radioactivity to account for the early-time UV luminosity of iPTF14atg, while not causing strong observable imprints around maximum light, requires a dedicated study with high-resolution simulations.

Alternatively, geometry effects could play a role. If, for example, IGEs and radioactive isotopes are confined to a narrow ring at the surface of the ejecta, an observer looking down a line of sight perpendicular to this ring could see additional luminosity from the surface radioactivity at early epochs, while later on the ring material will not provide an opacity source for radiation originating from the core of the ejecta. Such a geometry has been proposed by Diehl et al. (2014) to explain early-time γ-ray observations of SN 2014J obtained with the *Integral* satellite.

5 CONCLUSIONS

We have compared synthetic observables of state-of-the-art multi-dimensional explosion models to the light curves and spectra of the subluminous 2002es-like SN iPTF14atg. While the detection of an early-time UV spike in iPTF14atg was interpreted as evidence for a SD progenitor system in a previous analysis by Cao et al. (2015), we have difficulties explaining the spectral evolution of iPTF14atg within the SD progenitor channel from our models. Specifically, we find that the failed deflagration of a Chandrasekhar-mass WD, which could reproduce the observed luminosity of iPTF14atg quite well, has too fast evolving light curves compared to iPTF14atg and cannot account for the observed spectral features.

In contrast, we find reasonable agreement between the spectral evolution of a violent merger of two CO WDs with 0.90 and 0.76 $\rm M_\odot$, respectively, which had previously been suggested as progenitor for the 2002es-like SN 2010lp (Kromer et al. 2013b). Minor differences in the spectral features between this model, for which solar metallicity main-sequence progenitors were assumed, and iPTF14atg point at a mismatch in progenitor metallicity. Repeating the merger simulation for a progenitor system with sub-solar metallicity ($Z = 0.01 Z_\odot$), we find remarkably good agreement of the synthetic light curves and spectra with iPTF14atg for epochs after 10 d past explosion, suggesting a low-metallicity progenitor system for iPTF14atg.

At earlier epochs the flux level is slightly too low and our model cannot explain the early UV spike naturally. We argue that an additional energy source is required to explain the observed flux at these early epochs and discuss cooling of a shock heated CSM and surface radioactivity from a double detonation as possibilities

to account for the missing flux at early epochs with DD progenitors. In the light of recent studies (Raskin & Kasen 2013; Levanon et al. 2015), CSM interaction seems to be the most promising solution. Sophisticated radiation hydrodynamics simulations will be required to address this in more detail. Violent merger scenarios where an initial detonation of a He shell leads to the production of radioactive isotopes close to the surface of the ejecta, may also be a possible solution, if the peculiar surface composition will not leave a strong observable imprint around maximum light. A new generation of high-resolution WD merger models will be required, to investigate whether this is possible.

ACKNOWLEDGEMENTS

We gratefully acknowledge support from the Knut and Alice Wallenberg Foundation. The Oskar Klein Centre is funded by the Swedish Research Council. The work of RP and FKR is supported by the Klaus Tschira Foundation. RP also acknowledges support by the European Research Council under ERC-StG grant EXAGAL-308037. ST is supported by the Deutsche Forschungsgemeinschaft via the Transregional Collaborative Research Center TRR 33 'The Dark Universe'. AG and RA acknowledge support from the Swedish Research Council and the Swedish National Space Board. IRS was supported by the Australian Research Council Laureate Grant FL0992131.

The authors gratefully acknowledge the Gauss Centre for Supercomputing (GCS) for providing computing time through the John von Neumann Institute for Computing (NIC) on the GCS share of the supercomputer JUQUEEN (Stephan & Docter 2015) at Jülich Supercomputing Centre (JSC). GCS is the alliance of the three national supercomputing centres HLRS (Universität Stuttgart), JSC (Forschungszentrum Jülich), and LRZ (Bayerische Akademie der Wissenschaften), funded by the German Federal Ministry of Education and Research (BMBF) and the German State Ministries for Research of Baden-Württemberg (MWK), Bayern (StMWFK) and Nordrhein-Westfalen (MIWF).

REFERENCES

Arnett W. D., 1969, Ap&SS, 5, 180
Asplund M., Grevesse N., Sauval A. J., Scott P., 2009, ARA&A, 47, 481
Bianco F. B. et al., 2011, ApJ, 741, 20
Bloom J. S. et al., 2012, ApJL, 744, L17
Brown P. J. et al., 2012, ApJ, 753, 22
Cao Y. et al., 2015, Nature, 521, 328
Chomiuk L. et al., 2012, ApJ, 750, 164
Diehl R. et al., 2014, Science, 345, 1162
Dilday B. et al., 2012, Science, 337, 942
Faber S. M. et al., 2003, in Society of Photo-Optical Instrumentation Engineers (SPIE) Conference Series, Vol. 4841, Society of Photo-Optical Instrumentation Engineers (SPIE) Conference Series, M. Iye & A. F. M. Moorwood, ed., pp. 1657–1669
Filippenko A. V., 1982, PASP, 94, 715
Fink M. et al., 2014, MNRAS, 438, 1762
Fink M., Röpke F. K., Hillebrandt W., Seitenzahl I. R., Sim S. A., Kromer M., 2010, A&A, 514, A53
Foley R. J. et al., 2013, ApJ, 767, 57
Ganeshalingam M. et al., 2012, ApJ, 751, 142
Gezari S. et al., 2008, ApJL, 683, L131
Goobar A. et al., 2015, ApJ, 799, 106
Guillochon J., Dan M., Ramirez-Ruiz E., Rosswog S., 2010, ApJL, 709, L64
Hayden B. T. et al., 2010, ApJ, 722, 1691
Hillebrandt W., Niemeyer J. C., 2000, ARA&A, 38, 191
Höflich P., Khokhlov A., 1996, ApJ, 457, 500
Horne K., 1986, PASP, 98, 609
Iben, Jr. I., Tutukov A. V., 1984, ApJS, 54, 335
Jha S., Branch D., Chornock R., Foley R. J., Li W., Swift B. J., Casebeer D., Filippenko A. V., 2006, AJ, 132, 189
Kasen D., 2010, ApJ, 708, 1025
Kasen D., Röpke F. K., Woosley S. E., 2009, Nature, 460, 869
Kelly P. L. et al., 2014, ApJ, 790, 3
Kelson D. D., 2003, PASP, 115, 688
Kerzendorf W. E., Schmidt B. P., Asplund M., Nomoto K., Podsiadlowski P., Frebel A., Fesen R. A., Yong D., 2009, ApJ, 701, 1665
Khokhlov A. M., 1991, A&A, 245, 114
Kozma C., Fransson C., Hillebrandt W., Travaglio C., Sollerman J., Reinecke M., Röpke F. K., Spyromilio J., 2005, A&A, 437, 983
Kromer M. et al., 2013a, MNRAS, 429, 2287
Kromer M. et al., 2013b, ApJL, 778, L18
Kromer M., Sim S. A., 2009, MNRAS, 398, 1809
Kromer M., Sim S. A., Fink M., Röpke F. K., Seitenzahl I. R., Hillebrandt W., 2010, ApJ, 719, 1067
Law N. M. et al., 2009, PASP, 121, 1395
Levanon N., Soker N., García-Berro E., 2015, MNRAS, 447, 2803
Li W. et al., 2011, Nature, 480, 348
Liu Z.-W., Moriya T. J., Stancliffe R. J., 2015, MNRAS, 454, 1192
Lundqvist P. et al., 2015, A&A, 577, A39
Ma H., Woosley S. E., Malone C. M., Almgren A., Bell J., 2013, ApJ, 771, 58
Maeda K. et al., 2008, Science, 319, 1220
Maguire K. et al., 2011, MNRAS, 418, 747
Maguire K., Taubenberger S., Sullivan M., Mazzali P. A., 2016, MNRAS, 457, 3254
Maoz D., Mannucci F., Nelemans G., 2014, ARA&A, 52, 107
Margutti R. et al., 2012, ApJ, 751, 134
Marion G. H. et al., 2016, ApJ, 820, 92
Mazzali P. A., Chugai N., Turatto M., Lucy L. B., Danziger I. J., Cappellaro E., della Valle M., Benetti S., 1997, MNRAS, 284, 151
Mazzali P. A., Hachinger S., 2012, MNRAS, 424, 2926
Mazzali P. A., Röpke F. K., Benetti S., Hillebrandt W., 2007, Science, 315, 825
Nomoto K., 1980, Space Science Reviews, 27, 563
Nomoto K., 1982a, ApJ, 253, 798
Nomoto K., 1982b, ApJ, 257, 780
Nugent P. E. et al., 2011, Nature, 480, 344
Olling R. P. et al., 2015, Nature, 521, 332
Pakmor R., Edelmann P., Röpke F. K., Hillebrandt W., 2012a, MNRAS, 424, 2222
Pakmor R., Kromer M., Taubenberger S., Sim S. A., Röpke F. K., Hillebrandt W., 2012b, ApJL, 747, L10
Pakmor R., Kromer M., Taubenberger S., Springel V., 2013, ApJL, 770, L8
Patat F. et al., 2007, Science, 317, 924
Pérez-Torres M. A. et al., 2014, ApJ, 792, 38
Perlmutter S. et al., 1999, ApJ, 517, 565
Piro A. L., Chang P., Weinberg N. N., 2010, ApJ, 708, 598
Piro A. L., Morozova V. S., 2015, ArXiv e-prints

Rabinak I., Livne E., Waxman E., 2012, ApJ, 757, 35
Rabinak I., Waxman E., 2011, ApJ, 728, 63
Raskin C., Kasen D., 2013, ApJ, 772, 1
Reinecke M., Hillebrandt W., Niemeyer J. C., 2002, A&A, 386, 936
Riess A. G. et al., 1998, AJ, 116, 1009
Röpke F. K., Hillebrandt W., Schmidt W., Niemeyer J. C., Blinnikov S. I., Mazzali P. A., 2007, ApJ, 668, 1132
Ruiter A. J., Belczynski K., Sim S. A., Hillebrandt W., Fryer C. L., Fink M., Kromer M., 2011, MNRAS, 417, 408
Sahu D. K. et al., 2008, ApJ, 680, 580
Scalzo R. et al., 2014, MNRAS, 440, 1498
Schaefer B. E., Pagnotta A., 2012, Nature, 481, 164
Seitenzahl I. R., Cescutti G., Röpke F. K., Ruiter A. J., Pakmor R., 2013a, A&A, 559, L5
Seitenzahl I. R. et al., 2013b, MNRAS, 429, 1156
Shappee B. J., Stanek K. Z., Pogge R. W., Garnavich P. M., 2013, ApJL, 762, L5
Shen K. J., Guillochon J., Foley R. J., 2013, ApJL, 770, L35
Sim S. A., Sauer D. N., Röpke F. K., Hillebrandt W., 2007, MNRAS, 378, 2
Sim S. A. et al., 2013, MNRAS, 436, 333
Springel V., 2005, MNRAS, 364, 1105
Stephan M., Docter J., 2015, Journal of large-scale research facilities JLSRF, 1
Stritzinger M., Leibundgut B., Walch S., Contardo G., 2006, A&A, 450, 241
Tanikawa A., Nakasato N., Sato Y., Nomoto K., Maeda K., Hachisu I., 2015, ApJ, 807, 40
Taubenberger S., Kromer M., Pakmor R., Pignata G., Maeda K., Hachinger S., Leibundgut B., Hillebrandt W., 2013, ApJL, 775, L43
Taubenberger S. et al., 2009, MNRAS, 397, 677
Travaglio C., Hillebrandt W., Reinecke M., Thielemann F.-K., 2004, A&A, 425, 1029
Wang B., Han Z., 2012, New Astronomy Review, 56, 122
Webbink R. F., 1984, ApJ, 277, 355
Whelan J., Iben I. J., 1973, ApJ, 186, 1007
White C. J. et al., 2015, ApJ, 799, 52
Woosley S. E., Axelrod T. S., Weaver T. A., 1984, in Astrophysics and Space Science Library, Vol. 109, Stellar Nucleosynthesis, Chiosi C., Renzini A., eds., p. 263
Woosley S. E., Kasen D., 2011, ApJ, 734, 38
Woosley S. E., Kerstein A. R., Aspden A. J., 2011, ApJ, 734, 37
Woosley S. E., Weaver T. A., Taam R. E., 1980, in Texas Workshop on Type I Supernovae, Wheeler J. C., ed., pp. 96–112